

# Kinetics of In Vivo Proliferation and Death of Memory and Naive CD8 T Cells: Parameter Estimation Based on 5-Bromo-2'-Deoxyuridine Incorporation in Spleen, Lymph Nodes, and Bone Marrow<sup>1</sup>

Elisabetta Parretta,\* Giuliana Cassese,<sup>†</sup> Angela Santoni,<sup>\*\*‡</sup> John Guardiola,<sup>†</sup> Antonia Vecchio,<sup>§</sup> and Francesca Di Rosa<sup>2†‡</sup>

To study naive and memory CD8 T cell turnover, we performed BrdU incorporation experiments in adult thymectomized C57BL/6 mice and analyzed data in a mathematical framework. The following aspects were novel: 1) we examined the bone marrow, in addition to spleen and lymph nodes, and took into account the sum of cells contained in the three organs; 2) to describe both BrdU-labeling and -delabeling phase, we designed a general mathematical model, in which cell populations were distinguished based on the number of divisions; 3) to find parameters, we used the experimentally determined numbers of total and BrdU<sup>+</sup> cells and the BrdU-labeling coefficient. We treated mice with BrdU continuously via drinking water for up to 42 days, measured by flow cytometry BrdU incorporation at different times, and calculated the numbers of BrdU<sup>+</sup> naive (CD44<sup>int/low</sup>) and memory (CD44<sup>high</sup>) CD8 T cells. By fitting the model to data, we determined proliferation and death rates of both subsets. Rates were confirmed using independent sets of data, including the numbers of BrdU<sup>+</sup> cells at different times after BrdU withdrawal. We found that both doubling time and half-life of the memory population were ~9 wk, whereas for the naive subset the doubling time was almost 1 year and the half-life was roughly 7 wk. Our findings suggest that the higher turnover of memory CD8 T cells as compared with naive CD8 T cells is mostly attributable to a higher proliferation rate. Our results have implications for interpreting physiological and abnormal T cell kinetics in humans. *The Journal of Immunology*, 2008, 180: 7230–7239.

The T cell peripheral compartment is in constant homeostatic equilibrium, despite the entry of naive T cells from the thymus, the huge T cell expansion due to antigenic stimulation, and the death of short-lived effector T cells in the contraction phase following priming. In addition to the acute events involving small numbers of Ag-specific T cells, both naive and memory T cells undergo continuous cell division and death. T cell turnover occurs slowly in the presence of physiological T cell numbers and increases in case of T cell depletion, for example, in irradiated and/or immunodeficient individuals. Several molecules have been implicated in the homeostatic regulation of peripheral T cell numbers, including cytokines (i.e., IL-15, IL-7, etc.), MHC-peptides (either self- or cross-reactive peptides), and TNF/TNFR family members (1, 2).

We have previously demonstrated that mature CD8 T cells have a higher turnover in the bone marrow (BM)<sup>3</sup> as compared with

spleen and lymph nodes (LN) (3). BM CD8 T cells do not have a distinct differentiation stage enabling them with a greater capacity to proliferate, but rather are constantly stimulated within the organ (4). We characterized some of the molecular events occurring in CD8 T cells within the BM, such as increased phosphorylation of the signal-transducing molecules STAT-5 and p38 MAPK and reduced membrane expression of CD127, the IL-7R  $\alpha$ -chain (5). Both naive-phenotype CD44<sup>int/low</sup> and memory-phenotype CD44<sup>high</sup> CD8 T cells contain a higher percentage of proliferating cells in the BM than in spleen and LN (5). The important role played by the BM in mature CD8 T cell turnover becomes even more evident when the total numbers of proliferating CD8 T cells contained in the sum of spleen, LN, and BM are taken into account. This is especially the case for memory CD8 T cells, but occurs also for naive CD8 T cells, implying that the BM contribution cannot be neglected when the quantitative aspects of mature T cell turnover are assessed (3, 5, 6).

To estimate the rate of mature T lymphocyte turnover, dividing cells have been tracked in experimental animals by different methods, such as BrdU incorporation and CFSE labeling (7–9). Pivotal studies on the kinetics of BrdU labeling of T cells in spleen and LN of BrdU-treated mice have shown that naive and memory T cells are differently regulated, and that memory T cells have a higher turnover rate than naive T cells (7). Because of the potential toxicity of BrdU and CFSE, questions concerning T cell kinetics have been approached differently in humans, for example, by evaluation of telomere length and by administration of the nontoxic isotope deuterium (<sup>2</sup>H), which is incorporated in the DNA of dividing cells (8). Mathematical models

\*Department of Experimental Medicine, University of Rome "La Sapienza," Rome, Italy; <sup>†</sup>Institute of Genetics and Biophysics, "Adriano Buzzati-Traverso," Consiglio Nazionale delle Ricerche, Naples, Italy; <sup>\*\*</sup>Institute of Molecular Biology and Pathology, Consiglio Nazionale delle Ricerche, Rome, Italy; and <sup>§</sup>Istituto per le Applicazioni del Calcolo "M. Picone," Consiglio Nazionale delle Ricerche, Naples, Italy

Received for publication November 15, 2007. Accepted for publication March 25, 2008.

The costs of publication of this article were defrayed in part by the payment of page charges. This article must therefore be hereby marked *advertisement* in accordance with 18 U.S.C. Section 1734 solely to indicate this fact.

<sup>1</sup> This work was supported by Associazione Italiana per la Ricerca sul Cancro.

<sup>2</sup> Address correspondence and reprint requests to Dr. Francesca Di Rosa, Consiglio Nazionale delle Ricerche, c/o Department of Experimental Medicine, University of Rome "La Sapienza", viale Regina Elena 324, 00161 Rome, Italy. E-mail address: francesca.dirosa@uniroma1.it

<sup>3</sup> Abbreviations used in this paper: BM, bone marrow; LN, lymph node.

have been developed for the interpretation of T cell turnover data, tremendously improving the understanding of T cell kinetics under both physiological and pathological conditions, for instance, in HIV-infected patients (10, 11).

Because actively dividing T cells are localized in specialized “niches,” mostly in lymphoid organs, human studies suffer from the limitation of using blood as the only source of cells. Blood cell samples accurately reflect lymphoid periphery as long as cells distribute homogeneously among blood and lymphoid organs (12). Both naive and memory T cells are recirculating cells, nevertheless each of the two subsets is heterogeneous and contains cells with different proliferation rates. Two subpopulations of memory T cells have been described, central-memory and effector-memory, with the former having a higher self-renewal capacity than the latter (13); it is possible that blood contains a different proportion of the two memory subsets as compared with other lymphoid organs. Moreover, we and others have shown that both naive and memory CD8 T cells divide more extensively in the BM than in spleen and LN (3, 9). For a more comprehensive approach to T cell turnover kinetics, it is important to consider the contribution of different lymphoid organs to the total T cell population. In humans, it is estimated that  $\sim 7 \times 10^9$  T cells are present in blood, whereas LN, spleen, and BM contain, respectively,  $150 \times 10^9$ ,  $31 \times 10^9$ , and  $25 \times 10^9$  T cells. Taken together, these three organs contain  $>200 \times 10^9$  T cells, thus accounting for the great majority of total T cells (6).

In this manuscript, we examined the kinetics of naive and memory CD8 T cell turnover, taking into account the proliferating and total cells contained not only in spleen and LN, but also in the BM of thymectomized C57BL/6 (B6) mice. Although we cannot rule out that newly formed cells either immigrate from other organs or emigrate from the organs studied, we focused our analysis on spleen, LN, and BM based on the major contribution of these three organs to both CD8 T cell turnover and total CD8 T cell counts (3, 5, 6). We determined BrdU up-labeling and down-labeling curves by naive and memory CD8 T cells and interpreted the results in a mathematical framework.

## Materials and Methods

### Mice

C57BL/6J (B6) female mice which had been thymectomized at 4 wk, normal euthymic B6, and CD45.1-B6 female mice were all purchased from Charles River Laboratories. Mice were housed at our Institute Animal Facility, according to institutional guidelines. Sentinel mice were screened for seropositivity to Sendai virus, rodent coronavirus, and *Mycoplasma pulmonis* by the Murine Immunocomb test (Charles River Laboratories) and were found negative.

### BrdU treatment and staining

B6 mice were treated with 0.8 mg/ml BrdU (Sigma-Aldrich) in their drinking water (3). BrdU solution was prepared in sterile water, protected from light exposure, and changed daily. During the continuous labeling phase, thymectomized B6 mice received BrdU up to 42 days. As a control, euthymic B6 mice were treated with BrdU for 3 days in parallel. For the chase phase, thymectomized B6 mice received continuous treatment with BrdU for 14 days as above, then BrdU was replaced with normal water, and mice were analyzed at different times after treatment interruption. The night before the assay of chase experiments, control B6 mice were injected i.p. with 0.8 mg of BrdU in PBS. On the day of the assay, BM cells from these mice were used as positive BrdU staining control. BrdU staining was performed as previously described (3). In each staining experiment, the CD44 marker used to discriminate between naive and memory CD8 T cells was set based on CD44 expression of spleen, LN, and BM CD8 T cells from a young (2- to 3-month old) normal B6 mouse.

### CFSE labeling and adoptive transfer

Pooled cells from spleen and LN of B6 mice were either labeled with CFSE as previously described (14) or mock treated. Recipient CD45.1-B6 mice were injected i.v. with  $40 \times 10^6$  donor cells, either CFSE labeled or not. Adoptively transferred mice were injected i.p. with 150  $\mu$ g of poly:IC and treated with BrdU in their drinking water. After 3 days, mice were sacrificed and cells from spleen, LN, and BM analyzed by flow cytometry.

### Calculation of cell numbers

At different times after thymectomy, spleen, LN, and BM cells were counted by Trypan blue exclusion, after lysis of RBC, and the average value was calculated from three to five mice. For each time point, nucleated cell numbers contained in each organ were estimated based on recovered cell counts, as described (3). Memory and naive CD8 T cell numbers contained in each organ were calculated based on the corresponding percentages of CD44<sup>high</sup> and CD44<sup>int/low</sup> TCR<sup>+</sup> CD8<sup>+</sup> cells measured by flow cytometry and average values of nucleated cells in that organ. Similarly, for either memory or naive CD8 T cells, BrdU<sup>+</sup> cell numbers contained in each organ were calculated based on the corresponding percentages of BrdU<sup>+</sup> cells measured by flow cytometry and average numbers of cells for that organ.

### Mathematical analysis

To estimate the proliferation rate  $p$  and the death rate  $d$ , we fitted the functions (Equations 6–8) to our experimental data. Such functions were curves of the type  $x(t) = c_1 e^{c_2 t} + c_3 e^{c_4 t}$ , in which either parameter  $c_3$  or  $c_4$ ,  $c_4$  were unknown. We solved the corresponding nonlinear least squares problems with the help of the software Wolfram Mathematica and its routine nonlinear regress (Wolfram Research). The coefficient of determination ( $R^2$ ) values were calculated according to Ref. 15.

### Statistical analysis

Statistical analysis was performed by Students'  $t$  test. Differences were considered significant when  $p \leq 0.05$  and highly significant when  $p \leq 0.01$ .

## Results

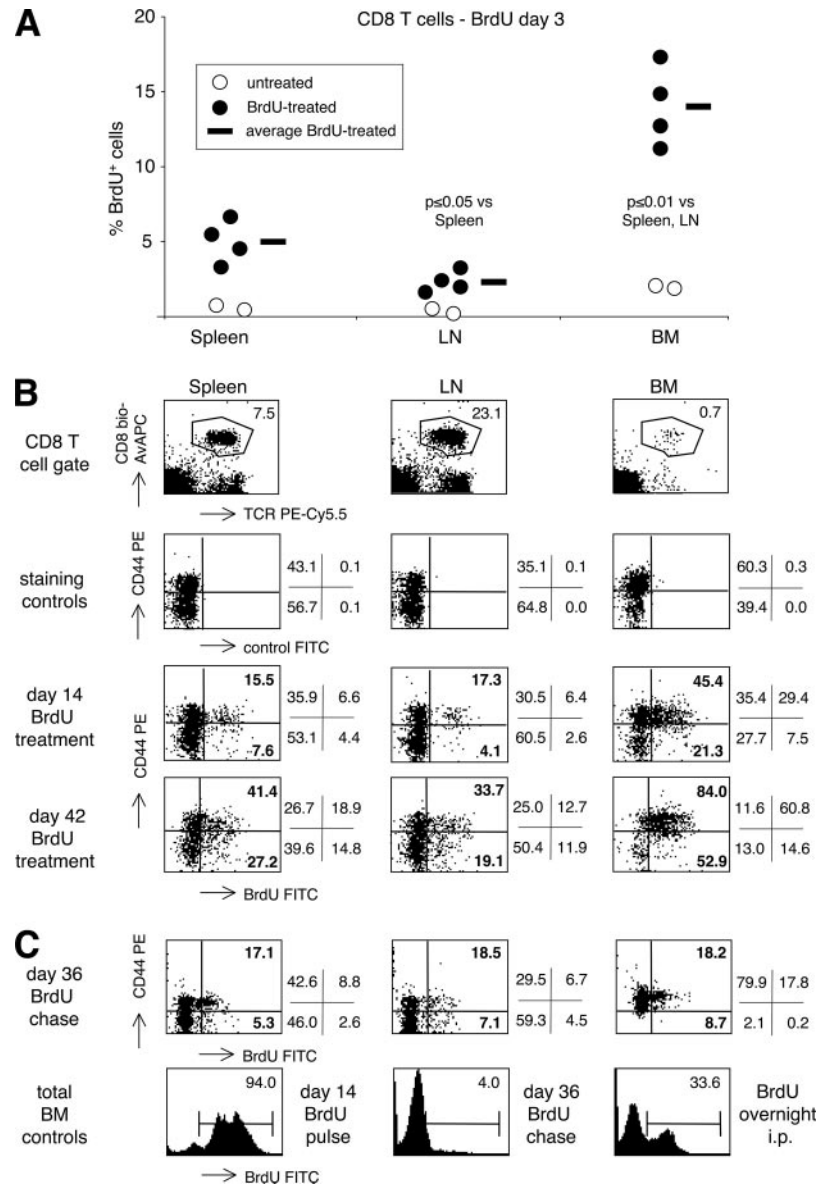
### BrdU incorporation experiments with thymectomized B6 mice

To study the kinetics of CD8 T cells in vivo, we treated adult thymectomized B6 mice with BrdU and analyzed cells from spleen, LN, and BM. By using thymectomized mice, we were able to prolong BrdU exposure up to 42 days without including CD8 T cells labeled in the thymus, which normally come out after day 3 (7).

During the continuous labeling period, BrdU was administered in the drinking water every day to a large group of thymectomized mice and a few of them were analyzed at different times of treatment (days 3, 14, 28, and 42). In agreement with our previous results in normal euthymic B6 mice (3), at day 3 the percentage of BrdU<sup>+</sup> CD8 T cells was higher in the BM than in the spleen and LN (Fig. 1A). We also analyzed some euthymic B6 mice in parallel with the thymectomized mice, and found no significant statistical difference at day 3 between the two groups (data not shown). Fig. 1B shows representative examples of cytometric analysis of spleen, LN, and BM CD8 T cells from mice treated with BrdU for 14 or 42 days. At any time tested, the BM contained the highest percentage of BrdU<sup>+</sup> CD8 T cells, either within naive (CD44<sup>int/low</sup>) or memory (CD44<sup>high</sup>) cell subset.

We also performed delabeling (chase) experiments. Mice were treated with BrdU for 14 days as above and then the treatment was stopped. Spleen, LN, and BM CD8 T cells were analyzed at different times of the die-away phase, i.e., at day 0 (corresponding to day 14 of BrdU labeling) and 4, 8, 17, and 36 days after interruption of BrdU treatment. Fig. 1C represents typical cytometric profiles of spleen, LN, and BM CD8 T cells at day 36, showing a slow decay of BrdU labeling in both naive and memory subset. As a control, for each mouse we analyzed total BM cells, showing a

**FIGURE 1.** BrdU labeling of CD8 T cells from B6 thymectomized mice. Single-cell suspensions were obtained from spleen, LN, and BM. After staining with anti-TCR-PECy5.5, anti-CD8 $\beta$ -biotin-streptavidin-allophycocyanin, and anti-CD44-PE plus either control-FITC or anti-BrdU-FITC, cells were analyzed by flow cytometry. **A**, BrdU<sup>+</sup> CD8 T cells in spleen, LN, and BM at day 3 of BrdU continuous labeling. In each organ the percentage of BrdU<sup>+</sup> cells in the TCR<sup>+</sup> CD8<sup>+</sup> population was determined after subtraction of background staining with control Ab. The panel summarizes the results obtained from three independent experiments. **B**, BrdU incorporation within naive and memory CD8 T cells during continuous labeling. The panels represent the cytometric analysis of spleen, LN, and BM at the indicated day of BrdU continuous labeling. In the *top panels*, the numbers represent the percentage of TCR<sup>+</sup> CD8<sup>+</sup> cells in the gated region. After gating on TCR<sup>+</sup> CD8<sup>+</sup> cells, naive and memory cells were discriminated based on CD44 expression. The marker was set based on CD44 expression of spleen, LN, and BM CD8 T cells from a young (2- to 3-mo old) normal B6 mouse, which was analyzed in parallel with samples from thymectomized mice. The numbers on the right of each panel indicate the percentage of cells in the corresponding quadrant. Bold numbers within quadrants represent the percentage of BrdU<sup>+</sup> cells within either CD44<sup>high</sup> (*top*) or CD44<sup>int/low</sup> (*bottom*) subset. **C**, BrdU incorporation within naive and memory CD8 T cells during the delabeling phase (chase). *Top panels*, The cytometric analysis of spleen, LN, and BM CD8 T cells at 36 days after interruption of a 14-day BrdU continuous treatment. *Bottom panels*, BrdU incorporation by BM total nucleated cells after the following BrdU treatments: 14 days of continuous labeling (*left*), 36 days of chase after a 14-day continuous labeling (*middle*), and overnight after a single BrdU i.p. injection (*right*). Numbers represent the percentages of BrdU<sup>+</sup> cells in the indicated region.



much faster BrdU decay. To control for BrdU staining on the day of the test, total BM cells from a B6 mouse pulsed overnight with BrdU were analyzed in parallel with samples from thymectomized B6 mice (Fig. 1C).

#### Analysis of the efficiency of the BrdU-labeling protocol

To evaluate the efficiency of our BrdU-based experimental approach in the detection of proliferating CD8 T cells, we compared the BrdU protocol with the CFSE method (3, 9, 14). Because BrdU protocol is based on the DNA incorporation of a nucleotide analog by the salvage pathway *in vivo*, it is likely to have a lower sensitivity than the CFSE method, in which cells are labeled *in vitro* with a cytoplasmic dye. Moreover, in contrast with the CFSE method, the BrdU protocol requires cell permeabilization and intranuclear staining (3, 16).

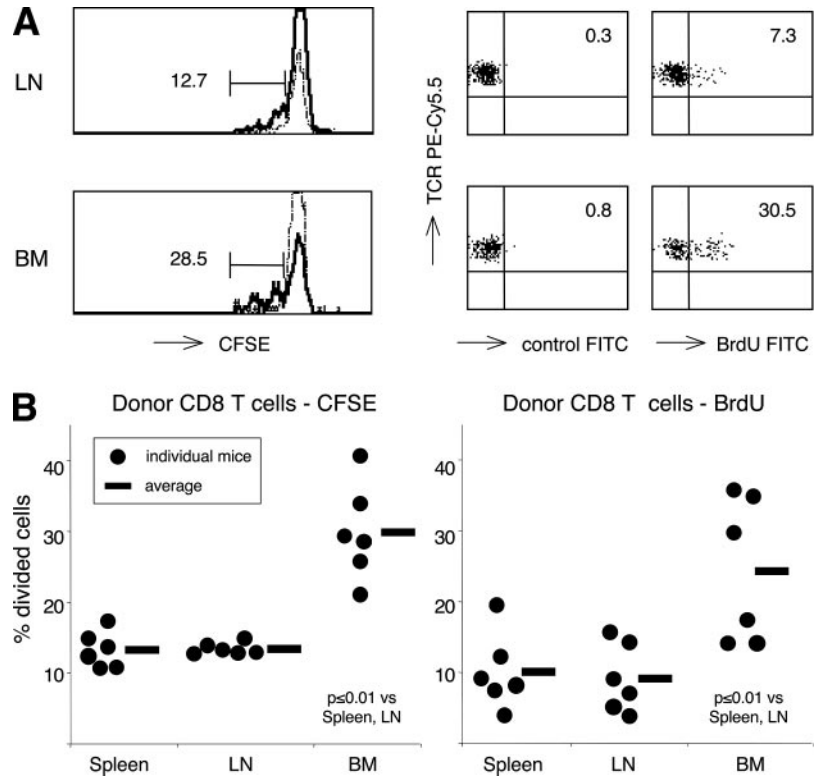
Equal numbers of either CFSE-labeled or unlabeled donor cells from spleen and LN of B6 mice were transferred into two groups of congenic B6-CD45.1 recipient mice. Mice were injected with poly:IC and treated every day with BrdU. After 3 days, spleen, LN, and BM cells were analyzed by flow cytometry and CD45.1<sup>-</sup> donor CD8 T cells were gated (9). As regards the CFSE method,

proliferation was measured based on CFSE fluorescence intensity. For the BrdU method, proliferation was determined by staining with anti-BrdU mAb FITC, after subtraction of background staining with control mAb. Representative cytometric profiles of LN and BM samples are shown in Fig. 2A and results are summarized in Fig. 2B.

In agreement with our previous observations (5), we found that poly:IC treatment-induced proliferation was higher in the BM than in either spleen or LN. Assuming that 100% of divided cells were detected by CFSE, for each organ we calculated the ratio between the percentage of divided cells measured by BrdU and the corresponding percentage measured by CFSE. We obtained the following ratios: spleen 0.8, LN 0.7, BM 0.8, suggesting that our BrdU protocol detected roughly 80% of those divided cells detected by CFSE (BrdU-labeling coefficient = 0.8).

In the above comparison between CFSE and BrdU protocol, both groups of mice were treated with BrdU, to avoid the possible confounding effect of BrdU treatment of only one group. We also performed additional experiments to check for the toxic effect of BrdU on CD8 T cell proliferation. Donor CFSE-labeled cells were transferred into CD45-congenic recipient,

**FIGURE 2.** BrdU-labeling protocol efficiency. After either CFSE labeling or mock treatment, pooled B6 spleen and LN cells were transferred into B6-CD45.1 recipient mice ( $40 \times 10^6$ /mouse). Mice received a single injection of poly:IC and were treated continuously with BrdU in drinking water. After 3 days, spleen, LN, and BM cells were stained with anti-TCR-Alexa 647, anti-CD8 $\beta$ -biotin-streptavidin-PerCpCy5.5, anti-CD45.1-PE and analyzed for either CFSE content or BrdU incorporation, as in Fig. 1. A, CFSE and BrdU staining examples. *Left histograms* show typical CFSE staining profiles of LN and BM CD45.1<sup>-</sup> donor CD8 T cells. Numbers indicate the percentages of divided donor CD8 T cells. *Right panels*, Typical BrdU staining profiles of LN and BM CD45.1<sup>-</sup> donor CD8 T cells. Numbers indicate the percentages of cells in the upper right quadrant. B, Comparison of donor CD8 T cell proliferation by BrdU and CFSE methods. The panels represent the percentages of divided donor CD8 T cells measured by CFSE (*left*) or BrdU (*right*). Values from individual mice are shown, as well as the average value for each organ. Both panels summarize the results obtained from three independent experiments.



which were injected with poly:IC and either treated or not with BrdU for 3 days. In both groups of mice, donor CD8 T cell proliferation was measured by the CFSE method in spleen, LN, and BM as above (data not shown). No statistically significant difference was found between corresponding organs from BrdU-treated and untreated mice ( $p$  value: spleen 0.76, LN 0.30, BM 0.89). Considering that, during the 3 days of BrdU administration, CD8 T cells divided extensively due to poly:IC treatment, our results suggest that BrdU does not affect CD8 T cell proliferation *in vivo* in our system. We also checked spleen cellularity after continuous BrdU treatment of thymectomized B6 mice for either 28 or 42 days and found no statistically significant difference between BrdU-treated and untreated mice ( $p$  value: 28 days 0.51, 42 days 0.64).

*The general mathematical model*

To study the kinetics of CD8 T cells and determine the proliferation and death rates of naive and memory cell subsets, we designed a general mathematical model to be separately applied to either naive or memory cell populations during the labeling and the delabeling periods.

The key point of our model is that at any time  $t$  we separate the CD8 T cell population (either naive or memory)  $y(t)$  into subpopulations depending on the number of divisions they perform until  $t$ . In our model,  $x_0(t)$  is the number of cells belonging to the considered population  $y(t)$  which have never divided during the time interval  $[0, t]$ , where  $t = 0$  is the initial time of our experiment;  $x_1(t)$  is the number of cells which divided once during the same interval and  $x_2(t)$  is the subpopulation which divided two or more times. The dynamics of these subpopulations is described by the following simple system of ordinary differential equations

$$\begin{cases} \frac{dx_0(t)}{dt} = -(p + d)x_0(t) \\ \frac{dx_1(t)}{dt} = 2px_0(t) - (p + d)x_1(t) \\ \frac{dx_2(t)}{dt} = 2px_1(t) + (p - d)x_2(t) \quad t \in [0, t_{final}] \\ x_0(0) = y(0) \\ x_1(0) = 0 \\ x_2(0) = 0 \end{cases} \quad (1)$$

in which  $y(0)$  is the number of cells at the beginning of the experiment,  $p$  and  $d$  are the per cell proliferation and death rate, respectively, and  $t_{final}$  is the final time of the experiment (in days).

The system (Equation 1) can be solved analytically and we obtain:

$$x_0(t) = y(0)e^{-(p + d)t} \quad (2)$$

$$x_1(t) = 2py(0)e^{-(p + d)t} \quad (3)$$

$$x_2(t) = y(0)e^{-(p + d)t}[e^{2pt} - (1 + 2pt)] \quad (4)$$

The sum of (Equations 2–4)  $x_0(t) + x_1(t) + x_2(t) = y(t)$  obeys to the classical exponential function

$$y(t) = y(0)e^{(p - d)t} \quad t \in [0, t_{final}] \quad (5)$$

Of course this reasoning can be further extended by separating  $y(t)$  into the sum of  $n$  subpopulations  $x_i(t)$ ,  $i = 0, \dots, n - 1$  each of which divided  $i$  times in the time interval  $[0, t]$ .

*Memory CD8 T cells kinetics: parameter estimation*

To estimate the proliferation and death rates of memory CD8 T cells, we used the data of BrdU continuous labeling experiments, taking into account the sum of BrdU<sup>+</sup> cells contained in spleen, LN, and BM.

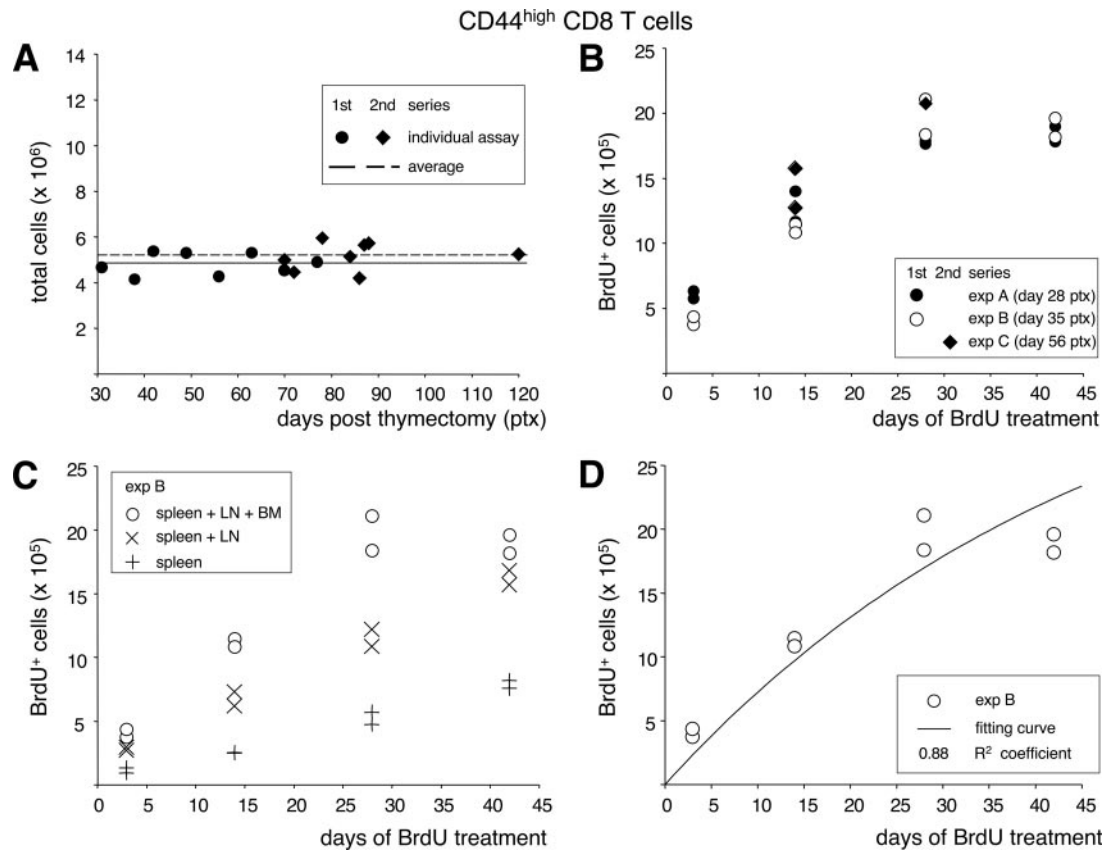


**FIGURE 3.** Analysis of BrdU labeling of CD44<sup>high</sup>CD8 T cells. **A**, Analysis of total CD44<sup>high</sup>CD8 T cell numbers after thymectomy. Experiments were performed in two independent series. For each series, female B6 mice were thymectomized at 4 wk and analyzed at different days after thymectomy. For each assay, three to five mice were killed and total memory CD8 T cell numbers from spleen, LN, and BM were calculated. Mean values of individual assays are shown, as well as the average values of the two series of experiments. **B**, BrdU<sup>+</sup> CD44<sup>high</sup>CD8 T cell numbers during BrdU continuous labeling. Mice were treated with BrdU in drinking water and analyzed at different times of BrdU labeling. Spleen, LN, and BM cells were stained as in Fig. 1. For each organ, the number of BrdU<sup>+</sup> memory CD8 T cells was calculated and the sum of spleen, LN, and BM values is shown for each mouse. Three independent experiments were performed (first series: experiments A and B; second series: experiment C), each starting at the indicated day after thymectomy. In the three experiments, for each day of analysis the SD was  $\leq 15\%$  of the average value. **C**, BrdU<sup>+</sup> CD44<sup>high</sup>CD8 T cell numbers in spleen, LN, and BM. The contribution of spleen, LN, and BM to the sum of BrdU<sup>+</sup> memory CD8 T cells is shown for each mouse in a typical experiment (experiment B). **D**, Plot of the fitting curve for CD44<sup>high</sup> CD8 T cells. The panel shows the sum of BrdU<sup>+</sup> memory CD8 T cells from spleen, LN, and BM of individual mice in a typical experiment (experiment B) and an example of the fitting curve  $M_L(t)$ . The corresponding value of the coefficient of determination ( $R^2$ ) is indicated. The calculated death rate value was  $d = 0.0104 \text{ days}^{-1}$ . The calculated death rate values without the BM were the following: spleen  $d = 0.0110 \text{ days}^{-1}$ ; spleen and LN  $d = 0.0087 \text{ days}^{-1}$ .

We first calculated the total numbers of memory CD8 T cells contained in spleen, LN, and BM of the thymectomized B6 mice, at different times after thymectomy. Fig. 3A shows that the total number of memory CD8 T cells was pretty stable over time, in two independent series of experiments (average value: first series  $4.8 \times 10^6$  cells, second series  $5.2 \times 10^6$  cells). This is expected, considering that the numbers of either memory or naive CD8 T cells are independently regulated (17) and thymectomy affects only the naive cells (18).

We then calculated the number of BrdU<sup>+</sup> memory CD8 T cells from three independent experiments of continuous labeling (experiments A, B, C), each started at a different time after thymectomy (days 28, 35, and 56, respectively). We analyzed BrdU incorporation at day 3, 14, 28, and 42 of continuous BrdU treatment (Fig. 3B). A similar increase of the number of BrdU<sup>+</sup> memory CD8 T cells was observed in the three experiments, suggesting that memory CD8 T cell proliferation was not influenced by the number of days after thymectomy, in the time frame analyzed. We observed a remarkable contribution of the BM to the number of BrdU<sup>+</sup> memory CD8 T cells (Fig. 3C).

We used the data of the above experiments to estimate the proliferation and death rates of memory CD8 T cells. We denote by  $M(t)$  the number of total memory CD8 T cells contained at time  $t$  in the sum of spleen, LN, and BM, where  $t = 0$  is the day of thymectomy. The population  $M(t)$  plays the role of  $y(t)$  given in (Equation 5). Considering that  $p = d$ , because the memory cell population is at a steady state, we have

$$M(t) = M(0)$$

in which  $t = 0$  is the day of thymectomy.

In our continuous labeling experiment, we denote by  $M_L(t)$  the number of BrdU<sup>+</sup> memory CD8 T cells contained at time  $t$  in the sum of spleen, LN, and BM, where  $t = 0$  is the initial time of BrdU labeling. The population  $M_L(t)$  is composed by subpopulations of cells which have divided once or more times during the interval  $[0, t]$ . By using our general model (Equation 1), we have

$$M_L(t) = bM(0)(1 - e^{-2dt}) \quad (6)$$

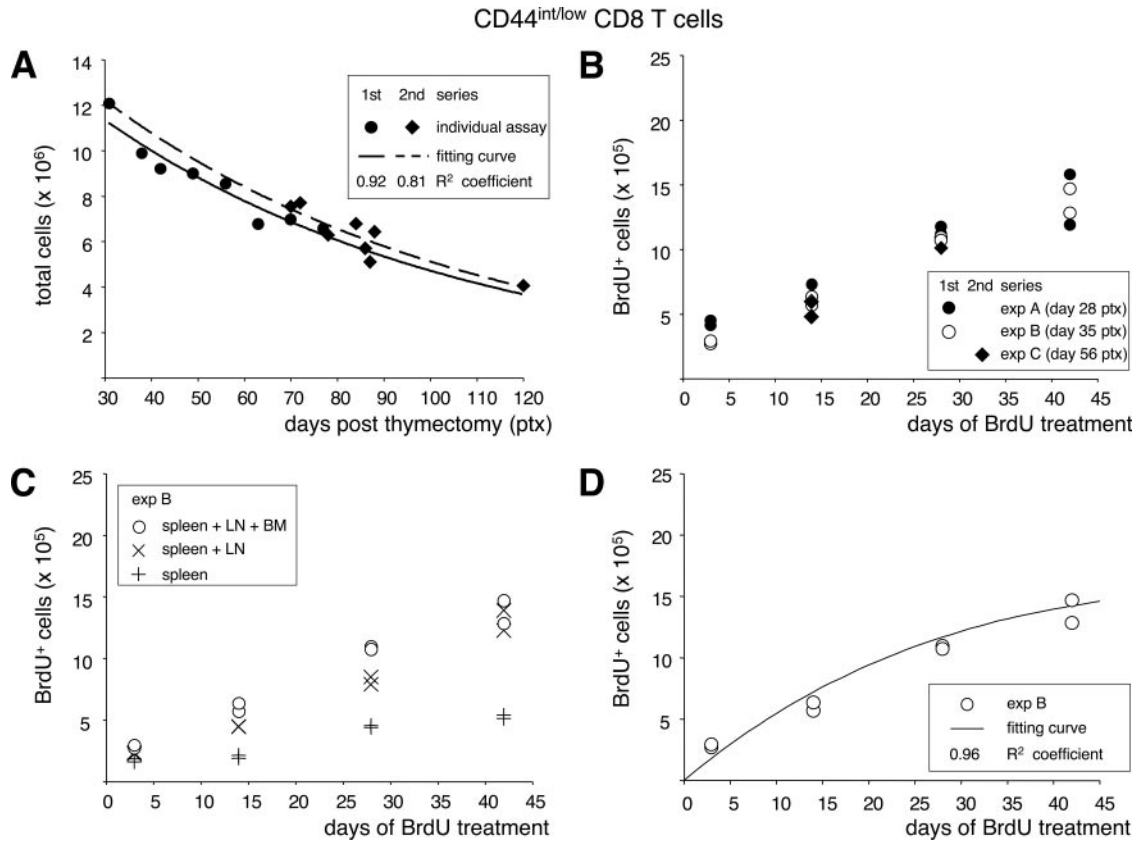


**FIGURE 4.** Analysis of BrdU labeling of CD44<sup>int/low</sup>CD8 T cells. *A*, Analysis of total CD44<sup>int/low</sup> CD8 T cell numbers after thymectomy. Experiments were performed as in Fig. 3 and total naive CD8 T cell numbers from spleen, LN, and BM were calculated. Mean values of individual assays are shown, as well as the fitting curve and the coefficient of determination ( $R^2$ ) for each series. *B*, BrdU<sup>+</sup> CD44<sup>int/low</sup> CD8 T cell numbers during BrdU continuous labeling. Experiments were performed as in Fig. 3 and the sum of BrdU<sup>+</sup> naive CD8 T cells from spleen, LN, and BM is shown for each mouse. In the three experiments, for each day of analysis the SD was  $\leq 20\%$  of the average value. *C*, BrdU<sup>+</sup> CD44<sup>int/low</sup>CD8 T cell numbers in spleen, LN, and BM. The contribution of spleen, LN, and BM to the sum of BrdU<sup>+</sup> naive CD8 T cells is shown for each mouse in a typical experiment (experiment B). *D*, Plot of the fitting curve for CD44<sup>int/low</sup> CD8 T cells. The panel shows the sum of BrdU<sup>+</sup> naive CD8 T cells from spleen, LN, and BM of individual mice in a typical experiment (experiment B) and an example of the fitting curve  $N_L(t)$ . The corresponding value of the coefficient of determination ( $R^2$ ) is indicated. The calculated rate values were  $p = 0.0024 \text{ days}^{-1}$  and  $d = 0.0150 \text{ days}^{-1}$ . The calculated rate values without the BM were the following: spleen  $p = 0.0025 \text{ days}^{-1}$ ;  $d = 0.0218 \text{ days}^{-1}$ ; spleen and LN  $p = 0.0025 \text{ days}^{-1}$ ;  $d = 0.0121 \text{ days}^{-1}$ .

in which  $t = 0$  represents the initial time of the continuous labeling experiment,  $b$  is the efficiency of our BrdU labeling method, and  $M(0)$  is the total number of memory cells contained in the three organs, which is constant. As we got an estimation of such a number (Fig. 3A), and also of the BrdU-labeling coefficient (Fig. 2B), the function (Equation 6) depends only on one free parameter, the death rate or  $d$ , which is equal to the proliferation rate or  $p$ . Fitting the function (Equation 6) to the data obtained from the three independent experiments, we estimated  $d$  for each experiment, obtaining the following values (corresponding confidence interval in parentheses): experiment A  $d = 0.0101 \text{ days}^{-1}$  (0.0075; 0.0126); experiment B  $d = 0.0104 \text{ days}^{-1}$  (0.0082; 0.0125); experiment C  $d = 0.0128 \text{ days}^{-1}$  (0.0100; 0.0156). The mean death rate of the three experiments is  $d = 0.0111 \text{ days}^{-1}$ . One example of the plot of the fitting curve  $M_L(t)$  is shown in Fig. 3D.

To confirm our estimations, we used the data from two novel independent experiments (respectively, day 14 and 28 continuous labeling). We plotted the curve given in (Equation 6), by using  $M(0)$  from each one of the two novel experiments, and by taking  $d$  as the mean value of experiments A–C ( $0.0111 \text{ days}^{-1}$ ). We found that the curves provided a good approximation of our day 14 as well as day 28 experimental data (data not shown). Moreover, the coefficient of determination ( $R^2$ ) values (15) were in both cases  $\geq 0.9$ , very close to the ones obtained during the fitting procedure of experiments A–C.

*Naive CD8 T cells kinetics: parameter estimation*

To study the kinetics of naive CD8 T cells, we calculated total and BrdU<sup>+</sup> cell numbers as described for the memory compartment. As expected in thymectomized mice, we found that the number of naive CD8 T cells declined exponentially after thymectomy in two independent series of experiments (Fig. 4A). Let  $N(t)$  be the number of naive cells playing the role of the population  $y(t)$  given in (Equation 5)

$$N(t) = N(0)e^{(p-d)t} \tag{7}$$

in which  $t = 0$  is the day of thymectomy.

Fitting (Equation 7) to the data obtained in two series of experiments, we get the following estimations of  $N(0)$  and  $p - d$

$$N(0) = 1.6543 \cdot 10^7 \quad p - d = -0.0126 \quad (\text{first series})$$

$$R^2 = 0.92$$

$$N(0) = 1.7739 \cdot 10^7 \quad p - d = -0.0125 \quad (\text{second series})$$

$$R^2 = 0.81$$

allowing us to approximate  $N(t)$  at any time  $t$ . By these means, we can estimate the number of total naive CD8 T cells at different

times after the thymectomy, corresponding to the initial times of our BrdU incorporation experiments.

We then calculated the numbers of BrdU<sup>+</sup> naive CD8 T cells from three independent experiments of continuous labeling, as described for the memory cells. The numbers of BrdU<sup>+</sup> naive CD8 T cells showed a gradual increase over time (Fig. 4B), less pronounced than for the memory population. Results were similar in the three experiments, suggesting that naive CD8 T cell proliferation was not influenced by the number of days after thymectomy, in the time frame analyzed. At each time point, BrdU<sup>+</sup> naive CD8 T cells were found not only in spleen and LN, but also in the BM (Fig. 4C).

According to our general model, Equation 1 provides

$$N_L(t) = bN(0)[e^{(p-d)t} - e^{-(p+d)t}] \quad (8)$$

in which  $N_L(t)$  represents the number of BrdU<sup>+</sup> naive CD8 T cells contained at time  $t$  in the sum of spleen, LN, and BM and  $t = 0$  represents the initial time of the continuous labeling experiment.

Observe that when  $p = d$ , Equation 8 coincides with Equation 6, as we have used a general mathematical model for both naive and memory CD8 T cells.

Once again, as we computed an estimation for  $N(0)$  and  $p - d$ , the above function (Equation 8) has only one free parameter, the death rate or  $d$ . Fitting our data from the three independent experiments, we calculate  $p$  and  $d$  as follows ( $d$  confidence interval are indicated in parentheses): experiment A  $p = 0.0024 \text{ days}^{-1}$ ,  $d = 0.0150 \text{ days}^{-1}$  (0.0146; 0.0153); experiment B  $p = 0.0024 \text{ days}^{-1}$ ,  $d = 0.0150 \text{ days}^{-1}$  (0.0147; 0.0154); experiment C  $p = 0.0018 \text{ days}^{-1}$ ,  $d = 0.0143 \text{ days}^{-1}$  (0.0141; 0.0145). An example of the plot of the fitting curve  $N_L(t)$  is shown in Fig. 4D.

We confirmed our estimates using novel data from day 14 and 28 continuous labeling experiments, as in the case of memory CD8 T cells, and again we obtained good agreement between the estimated curves and the novel data (data not shown) and  $R^2 \geq 0.9$ . Taken together, our results suggest that our mathematical model is correct for both memory and naive CD8 T cells.

#### Delabeling curves of memory and naive CD8 T cells: comparison of models with different division numbers

To further confirm the proliferation and death rates based on the BrdU continuous labeling experiments, we performed BrdU chase experiments (experiments D and E). In the chase experiments, mice were analyzed at different times after interruption of a 14-day BrdU treatment, i.e., at days 0, 4, 8, 17, and 36.

Fig. 5, A and B, show the numbers of BrdU<sup>+</sup> memory and naive CD8 T cells during the delabeling period. As a control for BrdU decay, total BM cells from each mouse were analyzed, showing a sharp decline of BrdU<sup>+</sup> cell numbers as soon as BrdU administration was stopped (Fig. 5C).

Along the same line of our previous mathematical analysis, starting from our general model (Equation 1), we get two different solutions for the delabeling curves of each CD8 T cell subset. If we assume that, in absence of BrdU, each divided labeled cell results in two unlabeled cells, we get

$$M_L(t) = M(0)e^{-2dt} \quad (9a, \text{ for memory cells})$$

$$N_L(t) = N(0)e^{-(p+d)t} \quad (9b, \text{ for naive cells})$$

in which  $t = 0$  represents the initial time of the delabeling experiment.

In the case that only after the first division—but not after the subsequent divisions—a labeled cell still yields two labeled daughter cells, we obtain

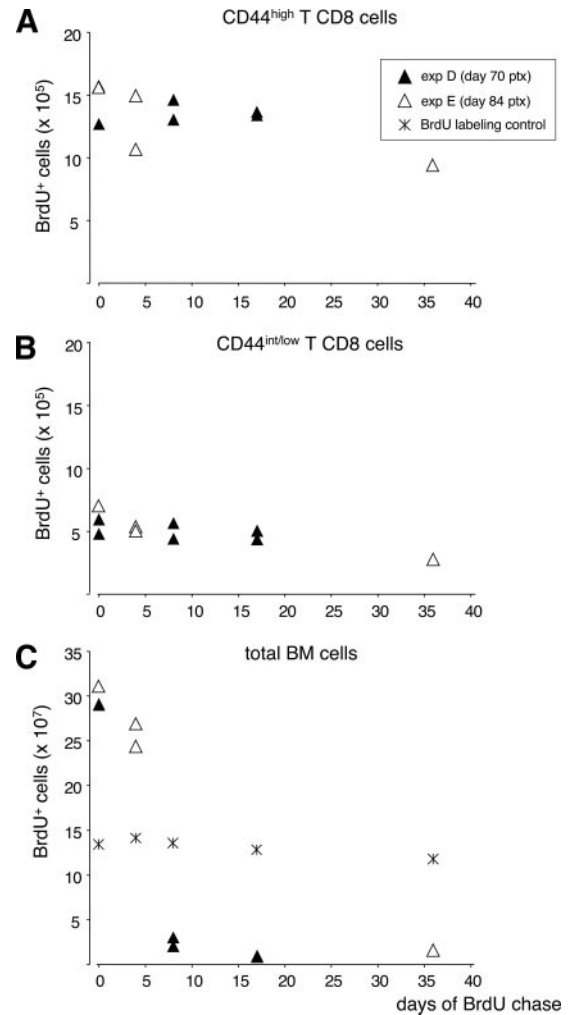


**FIGURE 5.** Analysis of BrdU delabeling of CD44<sup>high</sup> and CD44<sup>int/low</sup> CD8 T cells. After continuous treatment with BrdU in drinking water for 14 days, BrdU was replaced with normal water and mice were analyzed at different days of chase. A and B, BrdU<sup>+</sup> CD44<sup>high</sup> and CD44<sup>int/low</sup> CD8 T cell numbers during BrdU chase. Spleen, LN, and BM cells were stained and analyzed as in Fig. 1. For each organ, the number of BrdU<sup>+</sup> cells within memory (A) and naive (B) CD8 T cells was calculated and the sum of spleen, LN, and BM values is shown for each mouse. Two independent delabeling experiments were performed (second series: experiment D and E), each starting at the indicated day after thymectomy. C, BrdU<sup>+</sup> total BM cell numbers during BrdU chase. For each mouse, the percentage of BrdU<sup>+</sup> cells within total BM cells was measured and the corresponding number of BrdU<sup>+</sup> cells was calculated. BrdU-labeling controls were performed with normal B6 mice pulsed overnight with BrdU and examined in parallel with thymectomized B6 mice.

$$M_L(t) = M(0)e^{-2dt}(1 + 2dt) \quad (10a, \text{ for memory cells})$$

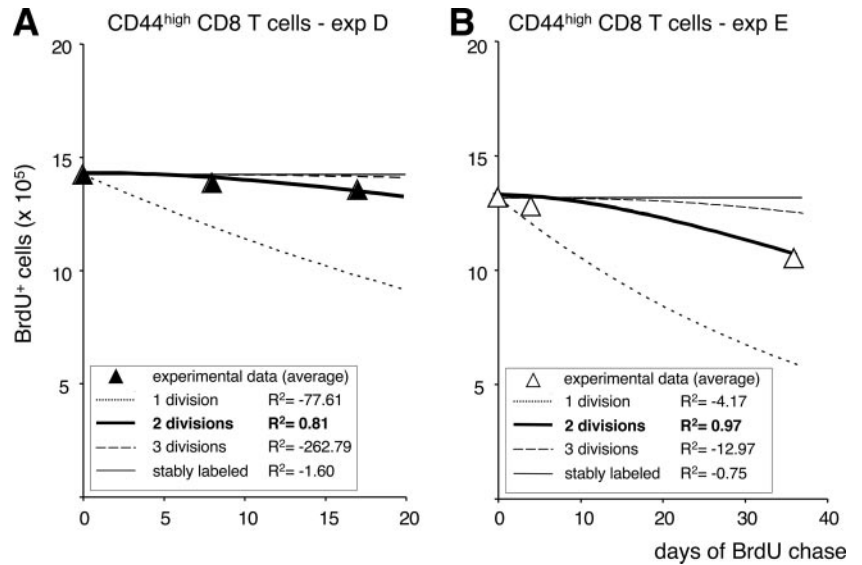
$$N_L(t) = N(0)e^{-(p+d)t}(1 + 2pt) \quad (10b, \text{ for naive cells})$$

in which  $t = 0$  represents the initial time of the delabeling experiment.

To choose between the two models (Equations 9 and 10, respectively), we compared the corresponding curves for each cell subset. These curves were obtained using  $p$  and  $d$  given by the mean values from continuous labeling experiments (A–C), whereas the average numbers of total and labeled cells were taken from chase experiments (either D or E).

As shown in Fig. 6 for memory CD8 T cells, the second formulation, i.e., the assumption that after the first division a labeled

**FIGURE 6.** Comparison of different delabeling theoretical curves of CD44<sup>high</sup>CD8 T cells. *A* and *B*, The functions representing different hypotheses of delabeling phase are plotted and compared with data from chase experiment D (*A*) and E (*B*). Each hypothesis is based on a different number of cell divisions after which BrdU labeling is lost (one to three divisions or never, i.e., cells stably labeled during the time of the experiment). For each curve, the corresponding value of the coefficient of determination ( $R^2$ ) is indicated.



cell yields labeled daughter cells and after the second division labeling is lost, is more appropriate. In addition to the curves corresponding to the two models (Equations 9 and 10, respectively), we also report in Fig. 6 the curves representing either the case of cells which lose the labeling only after the second division or the case of cells which remain labeled during the whole experiment. Similar results were found also in one of two chase experiments with naive CD8 T cells (data not shown).

Thus, our analysis of chase experiments confirms the estimation of  $p$  and  $d$  values obtained with continuous labeling experiments and suggests that in our system BrdU labeling is mostly lost by CD8 T cells upon the second division.

## Discussion

In contrast with previous studies on mature CD8 T cell turnover in mice (7, 19), we based our analysis of CD8 T cell kinetics on total BrdU-labeled naive and memory CD8 T cells contained in spleen, LN, and BM rather than only on percentages of BrdU-labeled cells in spleen and LN. We took this approach because: 1) the percentage of proliferating cells within either naive or memory CD8 T cells is higher in the BM than in spleen and LN (Fig. 1 and Refs. 3 and 5); 2) spleen, LN, and BM together contain the great majority of mature CD8 T cells in the body, making the sum of their CD8 T cells highly representative of the mature CD8 T cell pool (3, 5, 6).

We found that for naive CD8 T cells, on average, the proliferation rate was  $0.0022 \text{ days}^{-1}$  and the death rate was  $0.0148 \text{ days}^{-1}$ ; for memory CD8 T cells, both average rates were  $0.0111 \text{ days}^{-1}$ . Thus, every day  $\sim 1\%$  of memory CD8 T cells and  $0.2\%$  of naive CD8 T cells proliferate, and  $\sim 1\text{--}1.5\%$  of either memory or naive cells die. Within each subset, we considered that appearance and disappearance of BrdU-labeled cells were dependent only on cell proliferation and death. This accounts for the behavior of the majority of the cells in the time frame analyzed; nevertheless, it is possible that some cells shifted phenotype and others migrated out of the three lymphoid organs examined. Because CD44<sup>high</sup>CD8 T cell numbers were stable over time (Fig. 3A) and BrdU-labeling curves were very similar in independent experiments started at different days after thymectomy (Figs. 3B and 4B), we believe that phenotype shift did not greatly affect our results. The intermitotic or doubling time ( $t_2$ ), was  $\sim 315$  days for naive CD8 T cells and 63 days for memory CD8 T cells. Both subsets had a survival time or

half-life ( $t_{1/2}$ ) of more than a month (roughly 47 days for naive cells and 63 days for memory cells). Our results suggest that the higher turnover of memory CD8 T cells as compared with naive CD8 T cells is mostly attributable to a higher proliferation rate.

To investigate whether results would be different in the absence of BM contribution, we repeated our mathematical analysis taking into account either spleen cells alone or spleen and LN cells together. When the BM was not included and the analysis was performed on spleen and LN cells, we found slightly lower proliferation rates for memory cells and similar proliferation rates but lower death rates for naive cells. Nevertheless, for both cell subsets the fittings were still good and the difference between corresponding values with and without BM was not statistically significant (data not shown). This suggests that there was enough naive and memory CD8 T cell recirculation among the three lymphoid organs analyzed, so that cells which had incorporated BrdU in the BM contributed to BrdU-labeled cell numbers found in spleen and LN.

Mathematical models have been used for interpretation of mature CD8 T cell kinetics in different systems, including studies in humans with deuterium-labeled compounds and in monkeys with either deuterium-labeled compounds or BrdU, but there is still a big controversy on physiological turnover rates of naive and memory CD8 T cells (reviewed in Ref. 11). In rodents, in most cases, results have been interpreted intuitively rather than in a mathematical framework, making comparison with our results difficult (19–21). In contrast with our study, those lacking mathematical analysis do not analyze separately the contribution of proliferation and death rates to either BrdU up-labeling or down-labeling curves (7, 19). In one case, T cell turnover was examined in thymectomized rats using a mathematical formula, but only CD3<sup>+</sup> cells from secondary lymphoid organs were analyzed and the formula was applied to diabetes-prone BB rats and not to control healthy WF rats (22).

Among the few studies in humans in which separate analysis of naive and memory CD8 T cells was performed, those by McCune et al. (23) and Wallace et al. (24) are the most similar to ours in terms of doubling time estimation, with 112–204 days for naive CD8 T cells and 18–40 days for memory CD8 T cells. Recently, it has been suggested that the doubling times of both naive and memory CD8 T cells in humans have been underestimated so far—

due to short labeling times and insufficient time points of analysis—and they are much longer than previously thought (N. Vrisekoop, I. Den Braber, A. B. De Boer, A. F. C. Ruiters, M. T. Ackermans, S. N. Van der Crabben, E. H. R. Schrijver, G. Spierenburg, H. P. Sauerwein, M. D. Hazenberg, et al., submitted for publication, cited after Ref. 11). It is possible that in our system naive CD8 T cell proliferation rate was increased because we analyzed T cell turnover in thymectomized mice. However, we observed similar proliferation rates in experiments performed at different times after thymectomy, suggesting that naive CD8 T cell kinetics did not change in the time frame analyzed (BrdU labeling within the third month after thymectomy). It is expected that, at later times after thymectomy, a higher level of lymphopenia occurs, and the proliferation rate of naive CD8 T cells increases due to additional compensatory mechanisms.

Our results are very different from other mathematical analyses of CD8 T cell kinetics as concerns the estimation of death rate and survival time. In contrast with studies in humans and monkeys (25, 26), reporting a rapid loss of labeled CD8 T cells in the chase phase and high death rates (either using BrdU- or deuterium-labeled compounds), we found that after interruption of BrdU treatment, BrdU-labeled CD8 T cell numbers slowly declined, whereas the number of BrdU-labeled total BM cells steeply decreased. We obtained good fittings of the data with the mathematical equation used to describe the BrdU continuous labeling phase, provided that we applied the equation which takes into account a loss of BrdU labeling upon the second cell division. By such equation, we confirmed both the proliferation and the death rates obtained in the BrdU up-labeling studies.

With respect to experimental results, our data are similar to studies of BrdU die-away curves in rodents (7, 19) in which spleen and LN CD8 T cells were examined. The discrepant results in humans and monkeys vs rodents might be explained by the different organs analyzed (blood in primates vs lymphoid organs in rodents); it is possible that the rapid disappearance of blood-labeled CD8 T cells during the chase phase is mostly due to migration from bloodstream into tissues rather than to cell death (27). The rapid disappearance of BrdU-labeled cells from blood after BrdU withdrawal was found also when B cells were studied in sheep (28), suggesting that this phenomenon is related to the blood compartment and is consistent across species. Moreover, individual differences in CD8 T cell kinetics exist among both humans and monkeys (25, 26), due to genetic background and/or environmental factors, and in some individuals results are similar to ours, which have been obtained in inbred mice.

As regards mathematical analysis of the BrdU die-away curve, our study is different from the majority of the others, in which the progeny of BrdU-labeled cells was considered stably labeled (11). The few studies which took into account the possibility that BrdU dilution upon cell divisions leads to BrdU-labeled cell disappearance used different approaches than ours (16, 22). The advantages of our mathematical model are the following: 1) the number of cell divisions is considered in both continuous labeling and chase equations, so that a unique framework is used for analysis of results; 2) in the chase equation, it is possible to compare different curves, each based on a different number of cell divisions required for the loss of BrdU positivity, including the possibility that BrdU positivity is not lost in the time frame of the experiment. Thus, we do not assume a priori neither a fixed number of cell divisions necessary for BrdU loss (22), nor a constant fraction of labeled cells lost due to BrdU dilution (16).

A major concern in cell kinetics studies is cell heterogeneity, which may lead to the estimation of a lower proliferation rate as compared with death rate (29). Indeed, several studies have re-

ported a discrepancy between the two estimated rates and explained it either by the existence of an external source of cells or more convincingly by cellular heterogeneity (16, 25, 29); to have a more reliable estimate, it was proposed to calculate the “average turnover rate,” defined as the death rate averaged over all cell subpopulations (30, 31). We did not confirm in our system the common observation of a much higher rate of disappearance of labeled cells in the chase phase as compared with their accumulation in the labeling phase. Still, heterogeneity exists within the two cell subsets we analyzed, especially within memory CD8 T cells. We believe that, for each subset, we included similar proportions of cells with different turnover rates in either up-labeling and down-labeling experiments, because we took into account the sum of spleen, LN, and BM cells and administered BrdU for a sufficiently long time before chase. Moreover, we considered the possibility that during the chase phase labeled cells disappeared not only because they died but also because their label was lost upon cell division, making it unlikely that the death rate was overestimated in our model.

By our comprehensive approach, we were able to measure with good approximation the average proliferation and death rates within mouse naive and memory CD8 T cell subsets. Our results have implications for human studies, especially for the interpretation of abnormal T cell kinetics found in HIV-infected patients and other diseased individuals (23).

## Acknowledgments

We thank F. Castiglione, P. L. Lollini, and R. Pabst for reading the manuscript.

## Disclosures

The authors have no financial conflict of interest.

## References

1. Sprent, J., and C. D. Surh. 2002. T cell memory. *Annu. Rev. Immunol.* 20: 551–579.
2. Watts, T. H. 2005. TNF/TNFR family members in costimulation of T cell responses. *Annu. Rev. Immunol.* 23: 23–68.
3. Parretta, E., G. Casseese, P. Barba, A. Santoni, J. Guardiola, and F. Di Rosa. 2005. CD8 cell division maintaining cytotoxic memory occurs predominantly in the bone marrow. *J. Immunol.* 174: 7654–7664.
4. Di Rosa, F., and A. Santoni. 2002. Bone marrow CD8 T cells are in a different activation state than those in lymphoid periphery. *Eur. J. Immunol.* 32: 1873–1880.
5. Casseese, G., E. Parretta, L. Pisapia, A. Santoni, J. Guardiola, and F. Di Rosa. 2007. Bone marrow CD8 cells down-modulate membrane IL-7R $\alpha$  expression and exhibit increased STAT-5 and p38 MAPK phosphorylation in the organ environment. *Blood* 110: 1960–1969.
6. Di Rosa, F., and R. Pabst. 2005. The bone marrow: a nest for migratory memory T cells. *Trends Immunol.* 26: 360–366.
7. Tough, D. F., and J. Sprent. 1994. Turnover of naive- and memory-phenotype T cells. *J. Exp. Med.* 179: 1127–1135.
8. Hellerstein, M. K. 1999. Measurement of T-cell kinetics: recent methodologic advances. *Immunol. Today* 20: 438–441.
9. Becker, T. C., S. M. Coley, E. J. Wherry, and R. Ahmed. 2005. Bone marrow is a preferred site for homeostatic proliferation of memory CD8 T cells. *J. Immunol.* 174: 1269–1273.
10. Antia, R., V. V. Ganusov, and R. Ahmed. 2005. The role of models in understanding CD8<sup>+</sup> T-cell memory. *Nat. Rev. Immunol.* 5: 101–111.
11. Borghans, J. A., and R. J. de Boer. 2007. Quantification of T-cell dynamics: from telomeres to DNA labeling. *Immunol. Rev.* 216: 35–47.
12. Blum, K. S., and R. Pabst. 2007. Lymphocyte numbers and subsets in the human blood: do they mirror the situation in all organs? *Immunol. Lett.* 108: 45–51.
13. Sallusto, F., D. Lenig, R. Forster, M. Lipp, and A. Lanzavecchia. 1999. Two subsets of memory T lymphocytes with distinct homing potentials and effector functions. *Nature* 401: 708–712.
14. Di Rosa, F., and A. Santoni. 2003. Memory T-cell competition for bone marrow seeding. *Immunology* 108: 296–304.
15. Chatfield, C. 1988. *Problem Solving: A Statistician's Guide*. Chapman and Hall, London.
16. Bonhoeffer, S., H. Mohri, D. Ho, and A. S. Perelson. 2000. Quantification of cell turnover kinetics using 5-bromo-2'-deoxyuridine. *J. Immunol.* 164: 5049–5054.
17. Tanchot, C., and B. Rocha. 1995. The peripheral T cell repertoire: independent homeostatic regulation of virgin and activated CD8<sup>+</sup> T cell pools. *Eur. J. Immunol.* 25: 2127–2136.

18. Di Rosa, F., S. Ramaswamy, J. P. Ridge, and P. Matzinger. 1999. On the lifespan of virgin T lymphocytes. *J. Immunol.* 163: 1253–1257.
19. von Boehmer, H., and K. Hafen. 1993. The life span of naive  $\alpha/\beta$  T cells in secondary lymphoid organs. *J. Exp. Med.* 177: 891–896.
20. Rocha, B., C. Penit, C. Baron, F. Vasseur, N. Dautigny, and A. A. Freitas. 1990. Accumulation of bromodeoxyuridine-labeled cells in central and peripheral lymphoid organs: minimal estimates of production and turnover rates of mature lymphocytes. *Eur. J. Immunol.* 20: 1697–1708.
21. Zimmerman, C., K. Brduscha-Riem, C. Blaser, R. M. Zinkernagel, and H. Pircher. 1996. Visualization, characterization, and turnover of CD8<sup>+</sup> memory T cells in virus-infected hosts. *J. Exp. Med.* 183: 1367–1375.
22. Norwich, K. H., S. Ramanathan, and P. Poussier. 1999. Kinetics of T cell turnover following thymectomy. *Cell. Prolif.* 32: 195–201.
23. McCune, J. M., M. B. Hanley, D. Cesar, R. Halvorsen, R. Hoh, D. Schmidt, E. Wieder, S. Deeks, S. Siler, R. Neese, and M. Hellerstein. 2000. Factors influencing T-cell turnover in HIV-1-seropositive patients. *J. Clin. Invest.* 105: R1–R8.
24. Wallace, D. L., Y. Zhang, H. Ghattas, A. Worth, A. Irvine, A. R. Bennett, G. E. Griffin, P. C. Beverley, D. F. Tough, and D. C. Macallan. 2004. Direct measurement of T cell subset kinetics in vivo in elderly men and women. *J. Immunol.* 173: 1787–1794.
25. Mohri, H., S. Bonhoeffer, S. Monard, A. S. Perelson, and D. D. Ho. 1998. Rapid turnover of T lymphocytes in SIV-infected rhesus macaques. *Science* 279: 1223–1227.
26. Macallan, D. C., B. Asquith, A. J. Irvine, D. L. Wallace, A. Worth, H. Ghattas, Y. Zhang, G. E. Griffin, D. F. Tough, and P. C. Beverley. 2003. Measurement and modeling of human T cell kinetics. *Eur. J. Immunol.* 33: 2316–2326.
27. Macallan, D. C., D. Wallace, Y. Zhang, C. De Lara, A. T. Worth, H. Ghattas, G. E. Griffin, P. C. Beverley, and D. F. Tough. 2004. Rapid turnover of effector-memory CD4<sup>+</sup> T cells in healthy humans. *J. Exp. Med.* 200: 255–260.
28. Debaq, C., B. Asquith, P. Kerkhofs, D. Portetelle, A. Burny, R. Kettmann, and L. Willems. 2002. Increased cell proliferation, but not reduced cell death, induces lymphocytosis in bovine leukemia virus-infected sheep. *Proc. Natl. Acad. Sci. USA* 99: 10048–10053.
29. Asquith, B., C. Debaq, D. C. Macallan, L. Willems, and C. R. Bangham. 2002. Lymphocyte kinetics: the interpretation of labelling data. *Trends Immunol.* 23: 596–601.
30. De Boer, R. J., H. Mohri, D. D. Ho, and A. S. Perelson. 2003. Estimating average cellular turnover from 5-bromo-2'-deoxyuridine (BrdU) measurements. *Proc. Biol. Sci.* 270: 849–858.
31. De Boer, R. J., H. Mohri, D. D. Ho, and A. S. Perelson. 2003. Turnover rates of B cells, T cells, and NK cells in simian immunodeficiency virus-infected and uninfected rhesus macaques. *J. Immunol.* 170: 2479–2487.